Supplementary Information - Mimicking the hair surface for Neutron Reflectometry

Serena Cozzolino,[a,b] Philipp Gutfreund,[b] Alexei Vorobiev,[b,c] Anton Devishvili,[b,c] Andrew Greaves,[d] Andrew Nelson,[e] Nageshwar Yepuri,[f] Gustavo S. Luengo,[*d] and Mark W. Rutland[*a,g,h,i]

1 Production of d-dodecanol

Chemicals and reagents of the highest grade were purchased from Sigma-Aldrich (Sydney, Australia) and were used without further purification. Solvents were purchased from Sigma-Aldrich and Merck. NMR solvents were purchased from Cambridge Isotope Laboratories Inc. (MA, USA) and Sigma-Aldrich and were used without further purification. D_2O (99.8%) was supplied by AECL, Canada. Anhydrous dichloromethane, tetrahydrofuran and diethyl ether were obtained from a LC Technology Solutions Inc.
To a cold (0°C) solution of lauric-d23 (89%D, 16.0 g, 72 mmol) in anhydrous tetrahydrofuran (150 mL) was added a mixture of lithium aluminium deuteride (3.1 g) and lithium aluminium hydride (0.4 g) portion wise under a nitrogen atmosphere. The reaction mixture was brought to reflux and stirred for 16 hours. After cooling to 0°C, the reaction mixture was quenched by pouring it slowly onto crushed ice in a large beaker (Caution: addition must be done slowly to avoid excessive generation of hydrogen gas). The mixture was extracted with dichloromethane (3×75 mL) dried over sodium sulfate and concentrated *in vacuo*. Analytical thin-layer chromatography (TLC) was performed using Merck aluminium backed silica gel 60 F254 (0.2 mm) plates, which were visualised with bromocresol green stains. Flash column chromatography was performed using Merck Kieselgel 60 (230-400 mesh) silica gel, with the eluent mixture reported as the volume:volume ratio. Purification gave dodecanol-d25 (15.0 g) as a colourless liquid which solidified on cooling. ^{1}H NMR (400 MHz, Figure 1(a)), ^{13}C NMR (100.6 MHz, Figure S2) and ^{2}H NMR (61.4 MHz, Figure 1(b)) spectra were recorded on a Bruker 400 MHz spectrometer at 298 K. Chemical shifts, in ppm, were referenced to the residual signal of the corresponding NMR solvent. Deuterium NMR was performed using the probe's lock channel for direct observation.

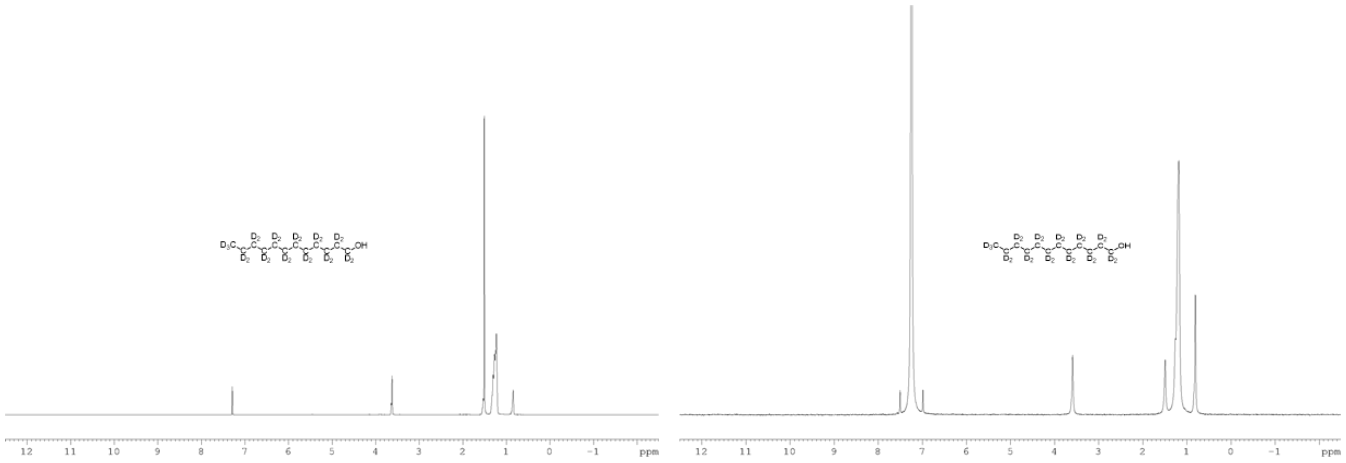

(a) (b)

Fig. S1 a) ^{1}H NMR (400 MHz) of dodecanol-d25 in $CDCl_3$. δ 3.60 (residual), 1.5 (residual), 1.50 (residual), 1.25 (residual), 0.82 (residual) ppm. b) ^{2}H NMR (61.4 MHz) of dodecanol-d25 in $CDCl_3$. δ 3.61 (2D, bs), 1.51 (2D, bs), 1.41-1.04 (20D, bm), 1.23 (12D, bs), 0.82 (3D, bs) ppm.

[a] *Division of Surface and Corrosion Science, School of Engineering Sciences in Chemistry, Biotechnology and Health, KTH Royal Institute of Technology, SE-100 44 Stockholm, Sweden.*
[b] *Institut Laue-Langevin, 71 avenue des Martyrs, CS 20156, 38042 Grenoble cedex 9, France.*
[c] *Department of Physics and Astronomy, Materials Physics, Uppsala University, SE-751 20 Uppsala, Sweden.*
[d] *L'Oréal Research and Innovation, 1 avenue Eugène Schueller, 93600 Aulnay-sous-Bois, France.*
[e] *Australian Nuclear Science and Technology Organisation, Australian Centre for Neutron Scattering, New Illawarra Rd, Lucas Heights, New South Wales, Australia.*
[f] *Australian Nuclear Science and Technology Organisation, National Deuteration Facility, New Illawarra Rd, Lucas Heights, New South Wales, Australia.*
[g] *Bioeconomy and Health Department, Materials and Surface Design, RISE Research Institutes of Sweden, SE-114 28 Stockholm, Sweden.*
[h] *School of Chemistry, University of New South Wales, Sydney, NSW 2052, Australia.*
[i] *Laboratoire de Tribologie et Dynamique des Systèmes, École Centrale de Lyon, 69134 Ecully CEDEX, France.*
[*] Corresponding authors. E-mail address: mark@kth.se (M. W. Rutland); gustavo.luengo@loreal.com (G. S. Luengo)

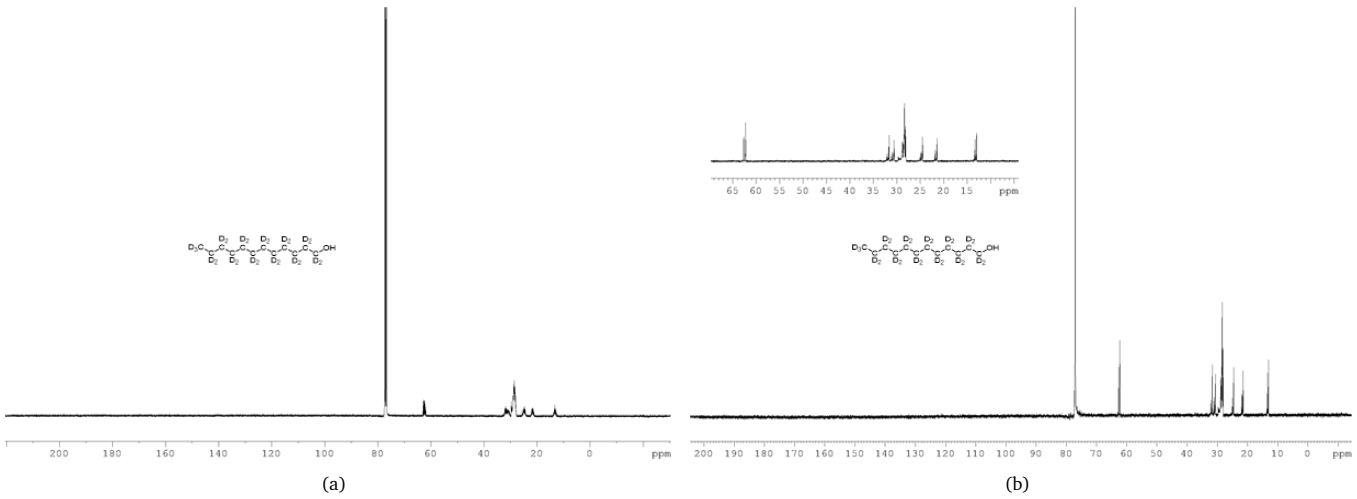

(a) (b)

Fig. S2 a) ^{13}C NMR (100.622 MHz) of dodecanol-d25 in $CDCl_3$. δ 13.34 (m), 21.6 (m), 24.5 (m), 28.5 (m), 30.8 (m)62.6 (m). b) ^{13}C {^{1}H,^{2}H} NMR (100.622 MHz) of dodecanol-d25 in $CDCl_3$, deuteration level at α-methylene calculated as 80%D[1]. δ 13.34, 21.6, 24.5, 28.5 (m), 30.72 (m) 31.72, 62.37 (d).

2 Neutron Reflectometry (NR) data fitting

A known issue with reflectometry data is the over-illumination of samples at very low angles of incidence. In this condition, the beam footprint is larger than the sample, causing a loss in reflected intensity at low values of the Q-vector. This can be normally corrected for during data reduction. The pySAred[2] software used here has, in fact, the option for over-illumination correction, which allows to flatten the low-Q region of the NR curve up to the critical edge. This correction is only possible, however, if the portion of the beam missing the interface is lost, e.g. absorbed by a beam stop. In the case of solid/liquid interfaces, as used here, this is usually not the case, as the over-illuminated beam fraction is reflected from the cell frame and detected together with the reflection of interest. Data fitting would then fail as this contribution is not constant along the whole Q-range of the dataset. In the high Q region, in fact, the angle of incidence is large enough for the neutron beam to hit only the studied interface justifying standard data analysis. On the other hand, the use of a single standard slab model could not fit the low Q region, but adding a second structure to consider mixed contributions to the signal would not result in a good fit either.

The effect of over-illumination was checked by measuring a test sample with two different slit sizes: the standard one used in the presented experiments and a much smaller one to ensure the neutron beam only shines on the sample throughout the whole theta-2theta scan. The results of this test are shown in Figure S3.

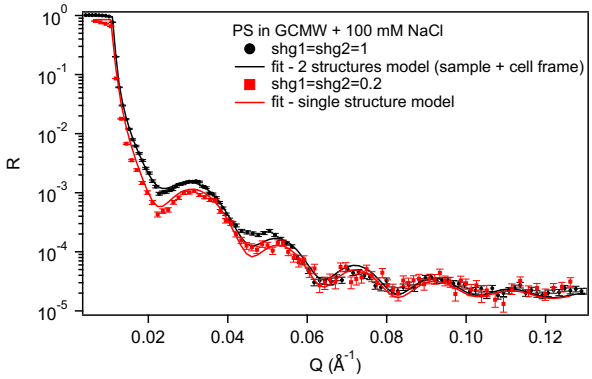

Fig. S3 Test sample scans at 2 slits sizes as indicated in the graph. Custom solid/liquid cell, sample surface: $65*65mm^2$, adhesion layer: chromium.

The sample (a functionalized gold-coated silicon block with a 120 Å thick chromium adhesion layer) was mounted in the same custom cell used for MBT and BT samples and filled with solvent (Gold Contrast-Matched Water with 100 mM NaCl). The two NR curves in Figure S3 show a clear difference around the first minimum ($Q \approx 0.02$ Å^{-1}). Fitting of the black curve required the addition of a second slab model, that considers the thiol surface facing air/cell frame instead of solvent (MixedReflectModel in RefNX - the bulk SLD for the second structure is considered to be 0 Å^{-2}). The scale factors for the two models indicate about 4% contribution from the second structure, and it can be seen that this causes an overestimation of the reflectivity at high Q, where the contribution disappears.

The curve obtained with smaller slits, instead, is fitted well by the application of one single slab model. The drawback of using such small slits, though, is the very low intensity of the detected signal (the fitted curve, in fact, had to be scaled to 85%), so that, to have good statistics at high Q, the measurement times would become extremely long.
Another test was done to check the influence of the chosen type of cell and substrate. We used for this a 50x50 solid/liquid cell (as the one employed for PS) and a substrate presenting a thin adhesion layer of titanium (Figure S4).

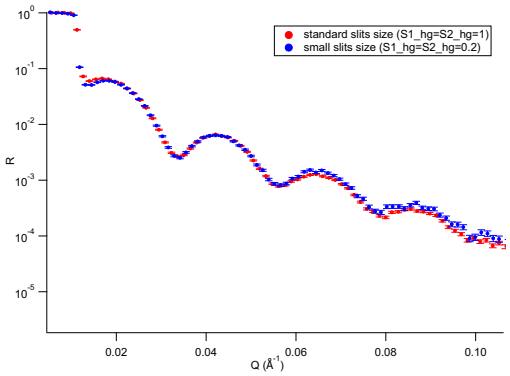

Fig. S4 Test sample scans at 2 slits sizes as indicated in the graph. Sample surface: $50*50mm^2$, adhesion layer: titanium.

A slight difference is visible around the first minimum, but definitely less dramatic than in the previous case. The measuring time in the case of the small slits was increased to have the same statistics at high Q as with bigger slits.
A simulation of a contribution from the cell frame shows that minima of the sample NR curve are aligned with maxima in the second structure (Figure S5). Due to the deeper minimum shown by the chromium containing substrate (Figure 5(a)), the effect is much bigger in this case.

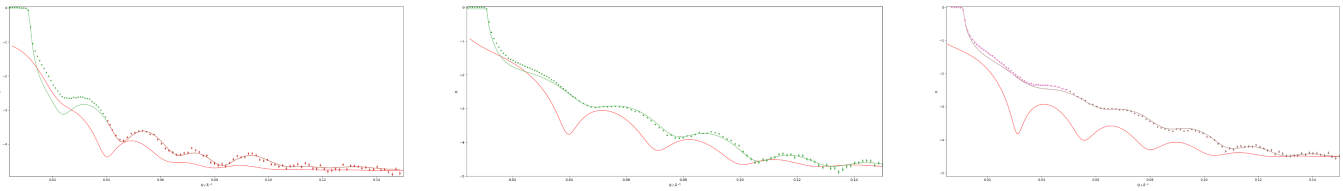

(a) (b) (c)

Fig. S5 Dotted line: NR data, green line: simulation of sample curve, red line: contribution from cell frame, for a) BT, b) MBT, c) PS. Simulated curves are arbitrary scaled.

NR data was fitted with the following procedure: first, the scattering length density (SLD) of the bulk solution is manually fitted from the critical edge of the curve, and similarly the background (not subtracted during data reduction) is manually adjusted. Then, data is fitted only in the Q range 0.04-0.15 Å^{-1}, setting up a slab model for the pure system of interest, and running a differential evolution plus MCMC analysis as described in the main text.
For MBT and BT, good fits (low Chi2, good fit by eye) were obtained by considering the SLD of the dry thiol and fitting layer thickness and roughness. In the case of PS, this procedure did not lead to a good fit, so the thiol SLD was added to the parameters to fit. Considering the expected dry SLD and the fitted value, we could define the percentage of hydration of the thiol layer. A similar method was used when fitting the adsorbed layer(s). In the case of the d-SDS/chitosan mixture, no prior assumption was made on the number of layers or their composition. A second slab was added if a good fit could not be obtained with one layer. In both cases (i.e., one or two adsorbed layers), the SLD value was fitted in the range from pure chitosan ($3.2*10^{-6}$ Å^{-2}) to pure d-SDS ($6.2*10^{-6}$ Å^{-2}). The value used for pure chitosan considers that each monomer has four exchangeable protons, so in GCMW three of them may be replaced by deuterons.
The obtained result (e.g., Figure 6(a)) is simulated on the whole curve (Figure 6(b)), checking whether variations in the experimental NR curves upon adsorption were reflected by differences in the simulated curves despite the non-overlapping of the two.

This method was used for most of the data presented in this work. However, a few improvements were needed in some cases, as described below.

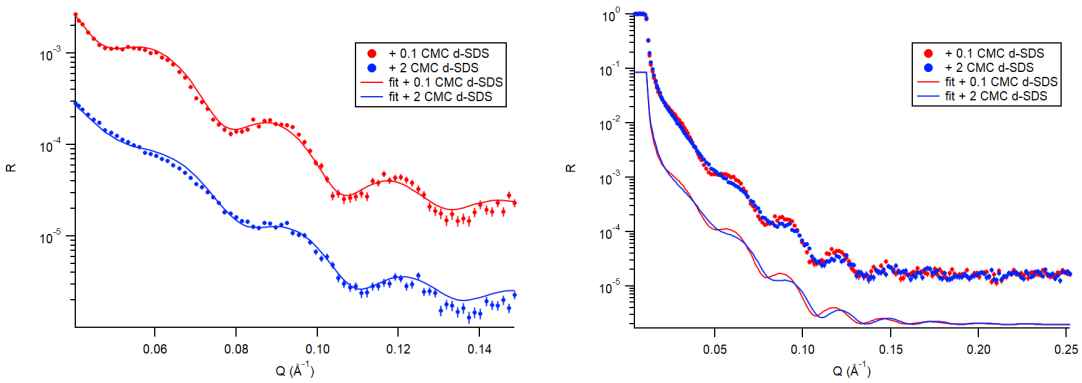

Fig. S6 NR data (dots) and fitted curve (lines) for MBT in the presence of 0.1 cmc and 2 cmc d-SDS, in GCMW and 100 mM NaCl. a) Fitted Q range. Data relative to the 2 cmc step was scaled by a factor of 0.1. b) Simulation over the full Q range. Simulated curves are scaled by a factor of 0.1.

2.1 PS

PS data (sample 1) was fitted for Q above 0.05 Å^{-1}, due to the smaller sample size that extended the cell frame contribution along the Q range. Figure 7(a) shows the fitted NR curve in the Q range from 0.04 to 0.15 Å^{-1}. The fitted curve visibly deviates from the NR data at low Q, which is compatible with the maximum in the simulated curve relative to cell frame contributions. To avoid this, another fit was performed shifting the minimum Q value to 0.05 Å^{-1} (Figure 7(b)).

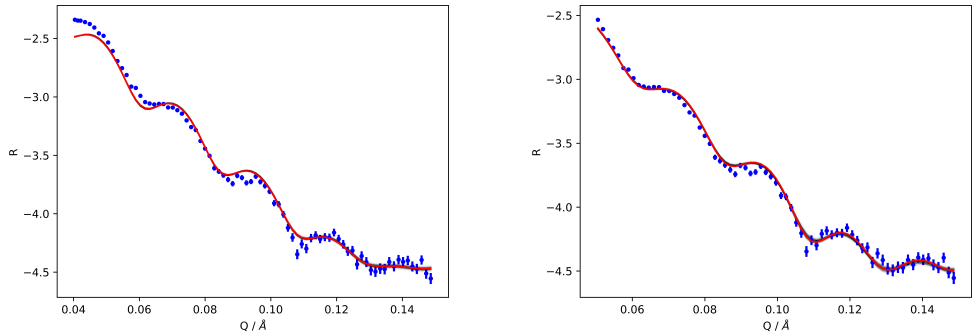

Fig. S7 NR data (dots) and fitted curve (lines) for PS in GCMW and 100 mM NaCl. a) Fitted Q range: 0.04-0.15 Å^{-1} b) Fitted Q range: 0.05-0.15 Å^{-1}.

The fit improves but still the corner plot resulting from MCMC sampling, shown in Figure S8, is not ideal. The values are not well centered in the squares, but given the physically reasonable constraints the analysis was considered good.

As a second check of the result, the fitted model was taken as starting point to fit the low Q range part (up to 0.05 Å^{-1}), using a mixed model to take into account contributions from a second structure due to the cell frame (MixedReflectModel in RefNX). Besides the scaling factors for the two structures, the only parameter that was fitted in this case was thiol thickness, as the obtained value from the high Q range fit was the lower limit selected for the parameter. Roughness also appears to hit the lower limit, but as its effect on the fitted curve was less evident, we chose to keep the fitted value. Results are in Figure S9.

The value for thiol thickness is here 8.4 Å instead of the 6.4 Å obtained at high Q. Figure 9(b) shows the two fitted curves extended to the full Q range. The agreement is fairly good, considering the 15% contribution from a second structure in the low Q region fit. Considering the error of 0.9 Å on the fitted parameter (see Table S1 in the next paragraph), PS layer thickness is better described by a mean value of about 7 Å, similarly to hydrophobic surfaces. Regarding sample 2, the PS layer was fitted either considering the theoretical SLD value, or adding the SLD parameter to the fit. The two results are similarly good, there is just a slight decrease in the chi-square value when fitting the SLD too. Specifically, considering the theoretical SLD of $1.13*10^{-6}$Å^{-2}, the thiol layer has a thickness of 7.7 $\pm$0.2 Å and roughness 2.01 $\pm$0.04 Å. In the other case, the SLD value decreases to 0.7 $\pm$0.9 $*10^{-6}$ Å^{-2}, while thickness and roughness become 7 $\pm$2 Å and 2 $\pm$3 Å, respectively. Such a SLD still has physical meaning but suggests that thiol density on the surface

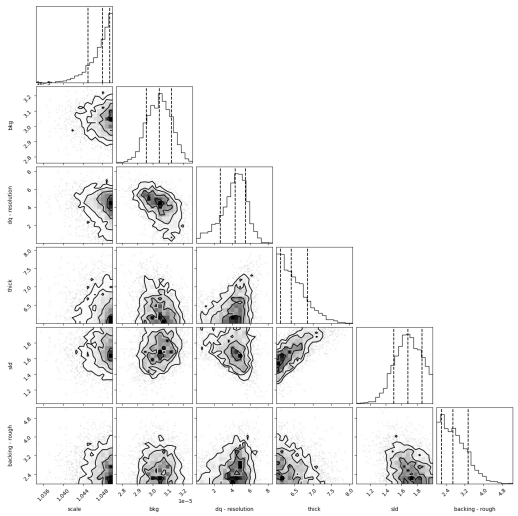

Fig. S8 Corner plot obtained from MCMC sampling of the data relative to PS in GCMW and 100 mM NaCl, fitted in the Q range 0.05-0.15 $Å^{-1}$.

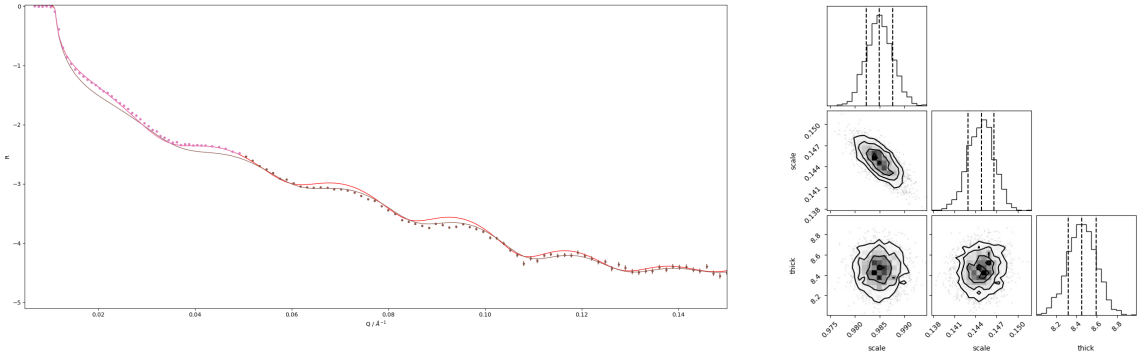

(a) (b)

Fig. S9 Fitting of NR data relative to PS in GCMW and 100 mM NaCl. a) Comparison between the two fitted curves for the high Q (brown) and low Q (red) regions b) Corner plot relative to data fitting in the low Q region (up to 0.05 $Å^{-1}$).

is lower than the bulk one (used to calculate the theoretical SLD value). It is worth noting, though, that errors on the fitted values are higher if the SLD is added to the fit. This is due to the correlation between thickness and SLD parameters. Nevertheless, the use of the second set of parameters to describe the thiol surface improved the fitting of the subsequently adsorbed layer, so it was chosen in the models for the next datasets.

2.2 Chitosan

Chitosan adsorption affects the NR signal in the low Q region more than in the high Q range. For this reason, in the steps where chitosan is present, the region up to 0.04 $Å^{-1}$ was also fitted separately. A mixed model was used, as previously mentioned. Results from the low Q and high Q regions of the curve were then compared and summed up. In the case of chitosan on the PS surface, different starting points for the fit gave different results, leading to the conclusion that the NR signal, for this system, is little affected by chitosan adsorption. The chitosan solution is injected after exposure of the surface to d-SDS and rinsing. The rinsing step shows the presence of a residue of d-SDS on the surface. As shown in Figure S10, rinsing the surface (with ≈ 5 cell volumes of GCMW and 100 mM NaCl) does not bring the curve exactly back to the starting point.

An exact description of this residual layer is difficult due to the small signal variation and the corresponding high uncertainty in fitting an adsorbed layer. Fitting the two regions separately (up to Q=0.05 $Å^{-1}$ and from this Q value on) results in slightly different thickness and roughness values. A comparison of the two models is shown in Figure S11, and corresponding parameters are in Table S1.

The difference in thickness for the two cases is within 16% of the smaller value. Using the model of the rinsing step at high Q to start fitting the data in the presence of chitosan, the result is quite similar to the previous, only a small decrease in the SLD value is

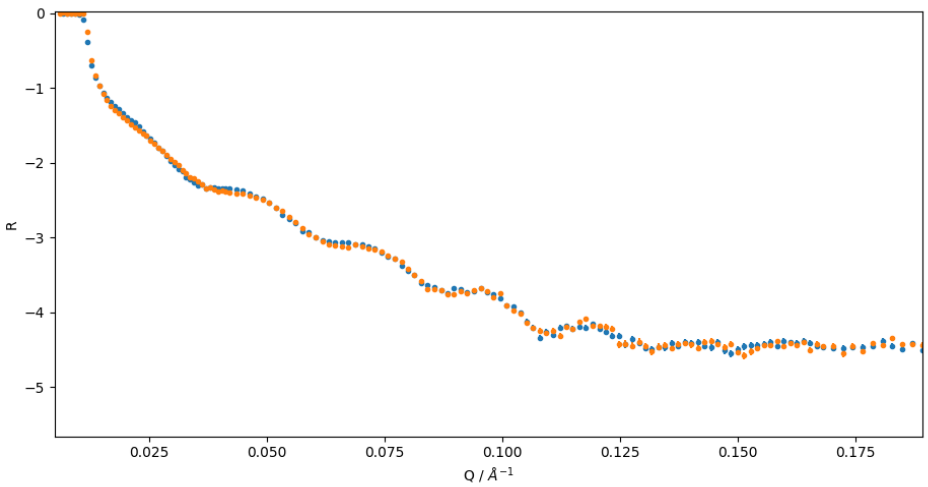

Fig. S10 Comparison between the NR curves relative to PS in GCMW and 100 mM NaCl before (blue line) and after (i.e., rinse - orange line) injection of d-SDS.

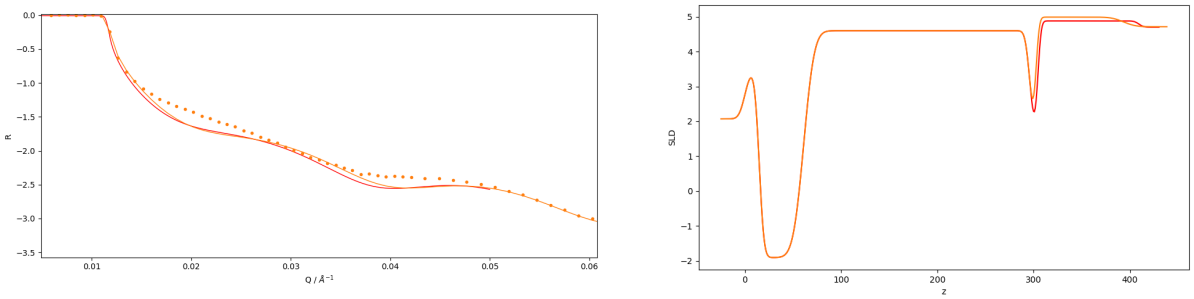

(a) (b)

Fig. S11 Fitting of NR data relative to rinsing of the PS surface with GCMW and 100 mM NaCl: comparison between the model used for Q<0.05 Å^{-1} (red - the single model corresponding to the system of interest, without cell frame contributions, is extracted and shown) and that for Q>0.05 Å^{-1}, extended in the low Q range (orange). a) Fitted curves b) SLD profiles.

indicative of the presence of chitosan (Figure S12).

The model was tested in the low Q region with the addition of the second structure describing cell contribution. Parameters were then manually varied to check the actual sensitivity of the model to the values fitted at high Q. Lowering the SLD value, to represent a $\approx$ 93% hydrated layer, and increasing the thickness of the layer (to have a similar layer to the one fitted on hydrophobic surfaces), results in a curve that fits equally well the NR data (Figure 13(a)). The validity of the previous fit of the rinsing step was then verified with the same method. In this case the fit is slightly worse when modifying the adsorbed layer parameters (Figure 13(b)). Parameters are in Table S1, in the order in which the tests were run.

Figure 14(a) shows the corner plot relative to rinsing of the PS surface after exposure to d-SDS (whose fitted parameters are in Table S1). It can be seen that the distribution corresponding to the roughness of the adsorbed layer is extended on the whole range, indicating a low influence of this parameter on the fitting. Table S1 shows a final row of results obtained by fitting the NR data of PS in the presence of chitosan in the low Q region. The SLD value was fixed to the previously chosen one. The thickness would reach the upper limit, so this was increased in successive steps up to 1000 Å, and similarly for the roughness. The resulting value looks fairly centered in the corner plot (Figure 14(b). *NB the scale in the plot is reduced to the range where solutions are found, but the fitting range started from 0 Å*), but as it does not look physically reasonable, the previous fit in the high Q region was chosen as representative of this step, with the caveat that the associated error is high.

2.3 Order of injection

Another test that was performed on the PS surface was to check whether exposure of the surface to chitosan changed its interaction with a 2 cmc d-SDS solution (the surface was rinsed in between, but as observed before rinsing did not remove the adsorbed layer). Surprisingly, as shown in Figure S15, the profile for adsorption of d-SDS from a 2 cmc solution is very similar before and after exposure

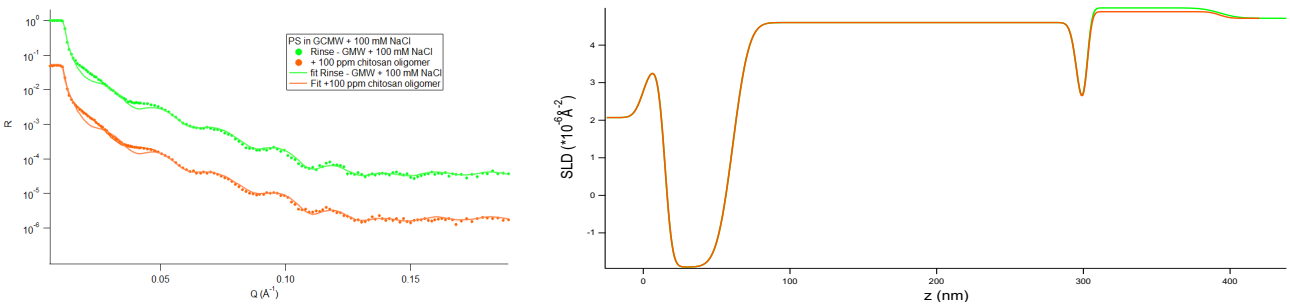

(a) (b)

Fig. S12 Fitting of NR data relative to rinsing of the PS surface with GCMW and 100 mM NaCl (green), and PS in the presence of 100 ppm chitosan (orange). a) Fitted curves b) SLD profiles.

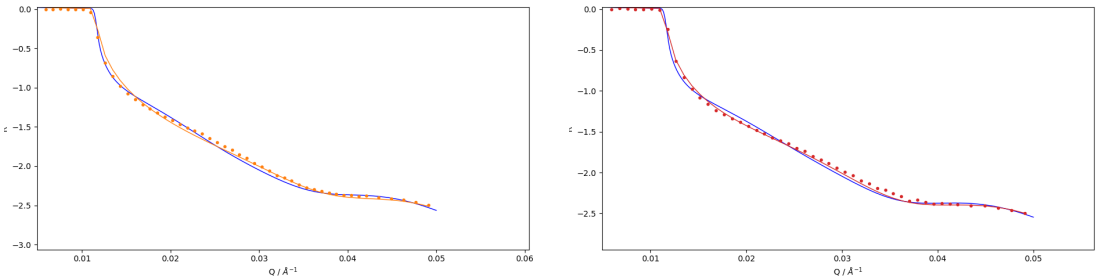

(a) (b)

Fig. S13 Fitting of PS NR data (orange) and simulated "chitosan-rich" layer (blue). a) PS after injection of 100 ppm chitosan b) PS after the rinsing step.

to chitosan.

The fitted thickness is slightly lower, 22 Å instead of the previous 28 Å and the hydration percentage, considering only d-SDS and GCMW solution as components, slightly decreases from 42% to 39%. Nevertheless, a concentration of 2 cmc does not appear enough, even in the presence of chitosan, to have a organized (bilayer) structure on PS.

Table S1 Fitted and simulated layer thickness, roughness and SLD values for PS layer, residual adsorbed layer in the rinsing step and adsorbed layer after injection of 100 ppm chitosan on the PS surface. Numbers in parenthesis indicate the error on the parameter value, equal to 2.5σ. The value in italics is fitted, but in a restricted range. In the case of fittings in the low Q region, only parameters corresponding to the model of interest are shown

	SLD ($*10^{-6}$Å^{-2})	Thickness (Å)	Roughness (Å)
PS layer - high Q fit	1.7 (0.4)	6.4 (0.9)	3 (1)
Rinse - high Q fit	4.99 (0.09)	91 (7)	10 (10)
Rinse - low Q fit	4.81 (0.01)	106 (11)	*5 (4)*
Chitosan - high Q fit	4.88 (0.07)	91 (7)	5 (7)
Chitosan/rinse - low Q, manually adjusted	4.6	200	10
Chitosan - low Q test fit	4.6	553 (54)	262 (44)

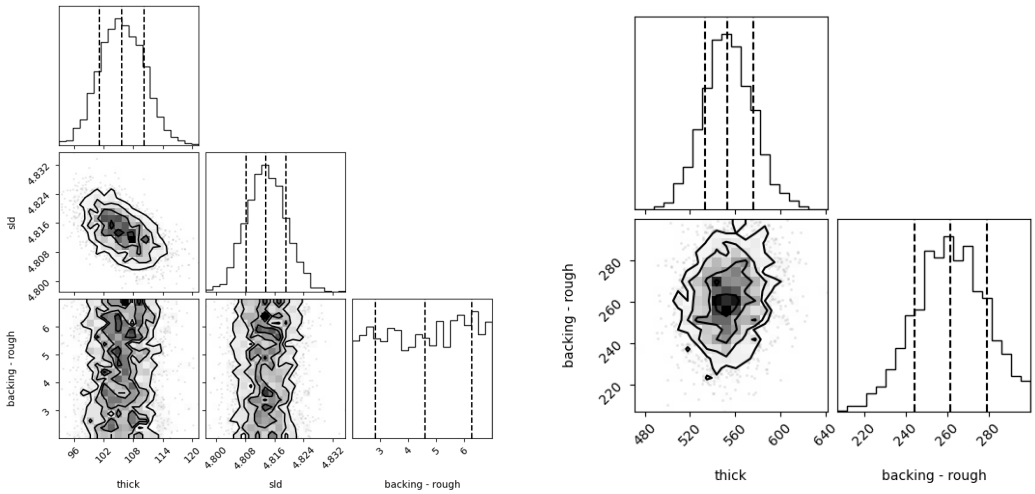

(a) (b)

Fig. S14 Corner plot corresponding to the NR data relative to: a) rinsing PS with GCMW and 100 mM NaCl after d-SDS adsorption, and b) PS in the presence of 100 ppm chitosan, both fitted in the region of Q<0.05 Å^{-1}.

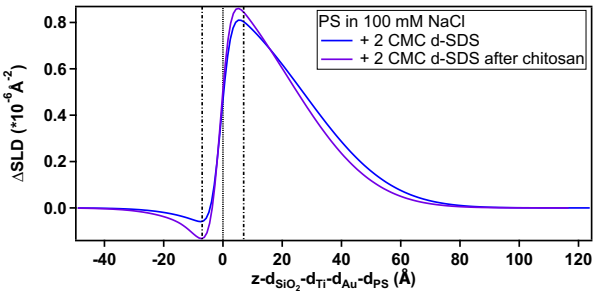

Fig. S15 Depth profile, after subtraction of the substrate profile, of d-SDS adsorbed on PS before or after chitosan as indicated on the graph. The dotted line at x = 0 indicates the PS/adsorbed layer interface, the dashed-dotted lines delimit PS roughness.

2.4 d-TTAB

d-TTAB was injected on PS after d- and h-SDS. Its adsorption on PS was difficult to define quantitatively. For both concentrations, i.e., 0.3 cmc and 6 cmc, the best fit is obtained considering one adsorbed layer. Surprisingly, this is better resolved at the lower d-TTAB concentration (Figure S16): the fit indicates the presence of an adsorbed layer of thickness 58 $\pm$4 Å, roughness $\approx$ 20 Å, and SLD 4.21 ($\pm$0.02)*10^{-6}Å^{-2} (meaning 18% d-TTAB, considering an SLD of 5.4*10^{-6}Å^{-2} for pure d-TTAB, and if the previous residue is not displaced). Instead, for the 6 cmc step, two populations of solutions are found, as shown in the SLD profile in Figure 17(b). After rinsing (Figure S18), no layer is adsorbed on the PS surface, suggesting that the previously added d-TTAB was able to remove the SDS residue. A tentative fit of one adsorbed layer results in an undefined corner plot (see Figure 18(b)), so this model was discarded.

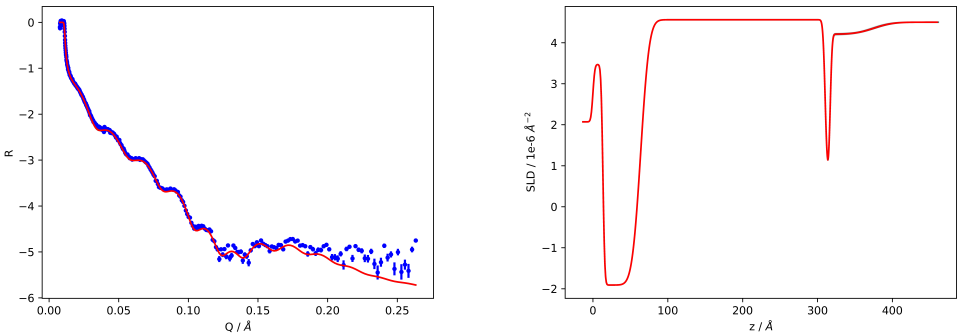

(a) (b)

Fig. S16 Fitting of NR data (blue dots) of PS in the presence of 0.3 cmc d-TTAB in GCMW and 100 mM NaCl. The shadowed part indicates the range of possible solutions. a) Fitted curve (red) b) SLD profile.

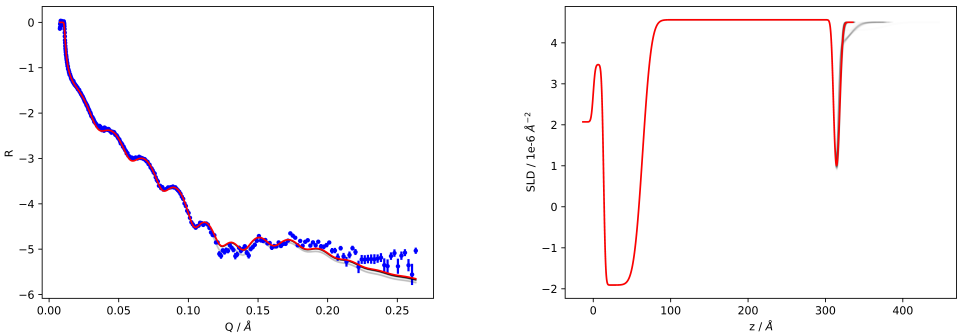

(a) (b)

Fig. S17 Fitting of NR data (blue dots) of PS in the presence of 6 cmc d-TTAB in GCMW and 100 mM NaCl. The shadowed part indicates the range of possible solutions. a) Fitted curve (red) b) SLD profile.

Instead, rinsing the PS surface after the SDS/TTAB mixture (discussed in the main text) does not fully remove the adsorbed layer, as shown in Figure S19. It removes, though, the well-defined surface layer, visible for adsorption of both SDS/TTAB and SDS/dodecanol. Thus, from Figures S18 and 19(b), it can be concluded that the SLD profiles shown in the main text for the two mixtures are indicative of adsorption from the injected solutions, so that the higher SLD values are not due to hydration but to a increasing contribution from adsorbed deuterated species.

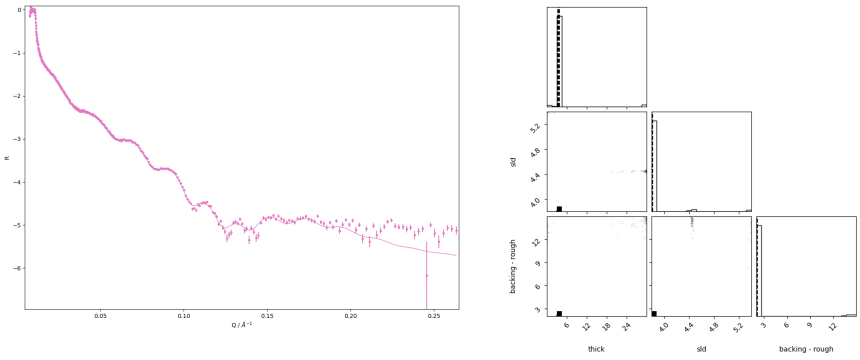

(a) (b)

Fig. S18 NR data of PS after rinsing d-TTAB, in GCMW and 100 mM NaCl. a) The pink solid line simulates the PS surface model in the absence of adsorbed layers b) corner plot resulting if one adsorbed layer is added and fitted.

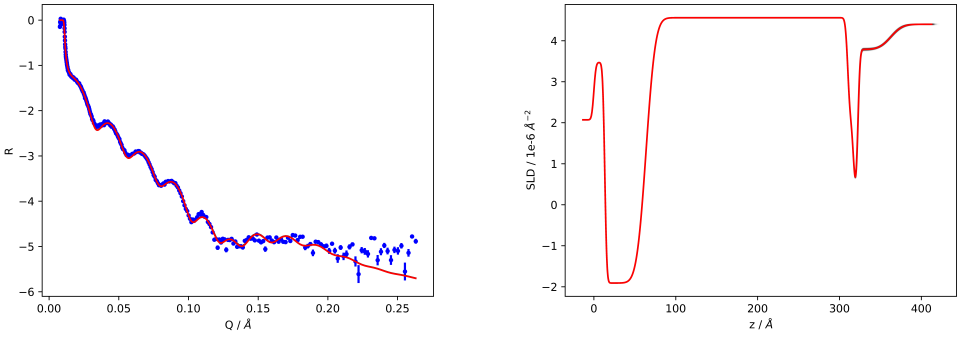

(a) (b)

Fig. S19 Fitting of NR data (blue dots) of PS in GCMW and 100 mM NaCl after exposure to h-SDS/d-TTAB. The shadowed part indicates the range of possible solutions. a) Fitted curve (red) b) SLD profile.

2.5 NR curves of the SLD profiles shown in main text

2.5.1 PS

Figures S20 and S21 show reduced data relative to the PS surface. Figures S22 to S27 show sample 1 fitted data (high Q region), while Figures S28 to S33 are from sample 2 (whole Q-range fit). Corresponding parameters are in Tables S2 and S3, respectively. *Note on the 20 cmc SDS steps.* The fitting in Figure S29 corresponds to a model with three adsorbed layers. A one-layer model gave a pretty good fit, but as more data points/a larger Q-range were available (compared to Figure 23(a), where a multilayer model would likely result in overfitting), a more detailed description was tested. The quality of the fit improved, but the SLD of the third layer had to be constrained to the theoretical value for d-SDS, $6.2*10^{-6}$Å^{-2}. If added to the fitting parameters, in fact, the result would suggest a thicker, highly hydrated structure in the third layer and the first two slabs would not be modified, but the quality of the fitting would be lower. The three-layer structure collapses to two layers when d-SDS is replaced by h-SDS.

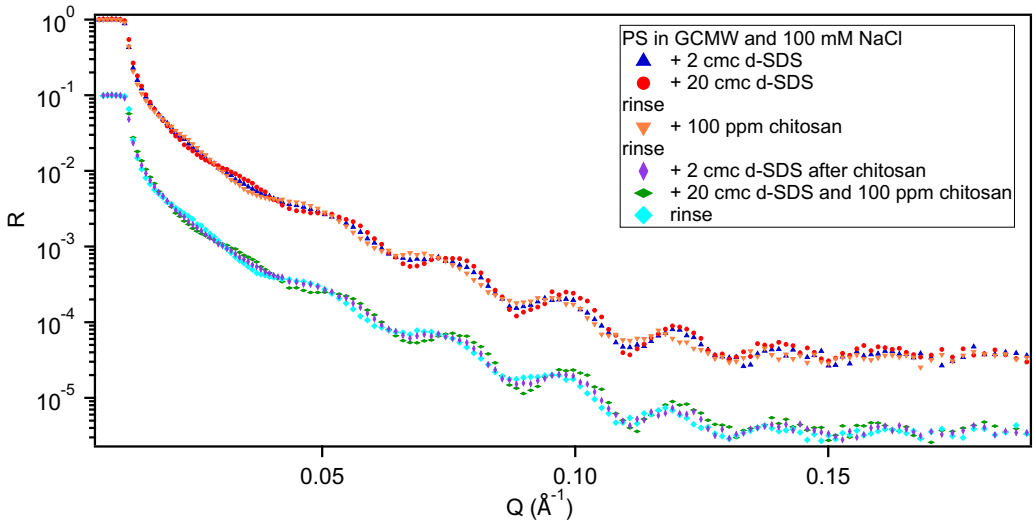

Fig. S20 Reduced NR curves relative to PS in GCMW and 100 mM NaCl in the presence of the molecules indicated in the graph. The second group of curves is scaled by a factor of 0.1.

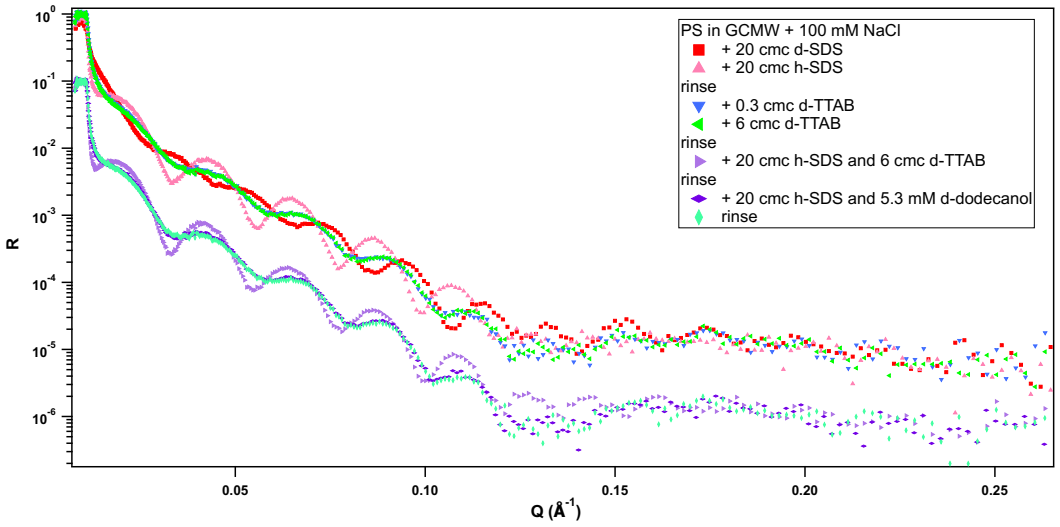

Fig. S21 Reduced NR curves relative to PS in GCMW and 100 mM NaCl in the presence of the molecules indicated in the graph. The second group of curves is scaled by a factor of 0.1.

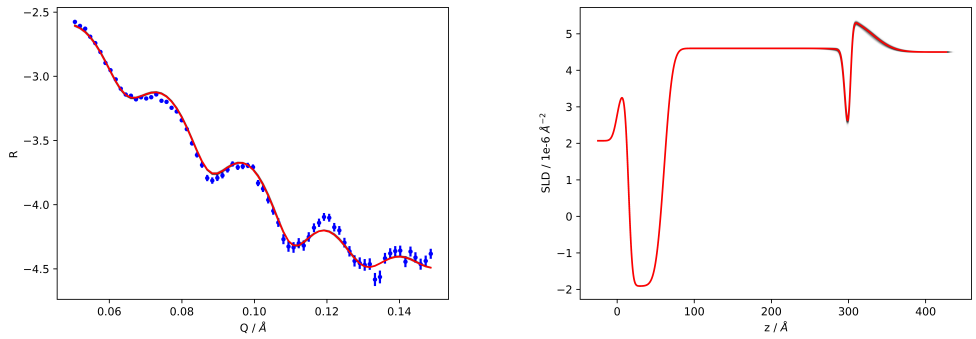

(a) (b)

Fig. S22 Fitting of NR data (blue dots) of PS in the presence of 2 cmc d-SDS in GCMW and 100 mM NaCl. The shadowed part indicates the range of possible solutions. a) Fitted curve (red) b) SLD profile.

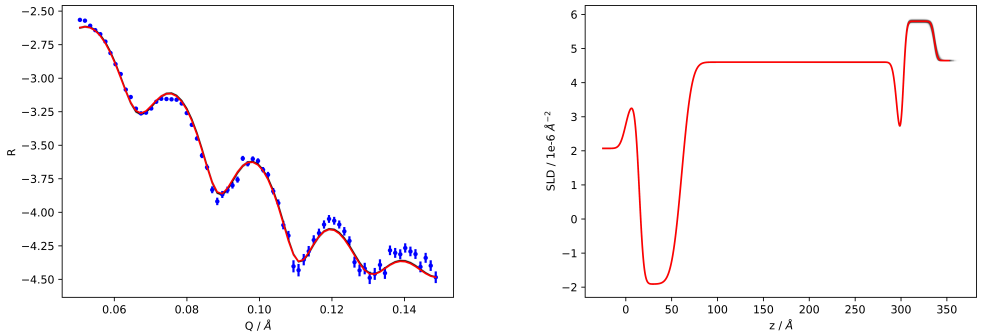

(a) (b)

Fig. S23 Fitting of NR data (blue dots) of PS in the presence of 20 cmc d-SDS in GCMW and 100 mM NaCl. The shadowed part indicates the range of possible solutions. a) Fitted curve (red) b) SLD profile.

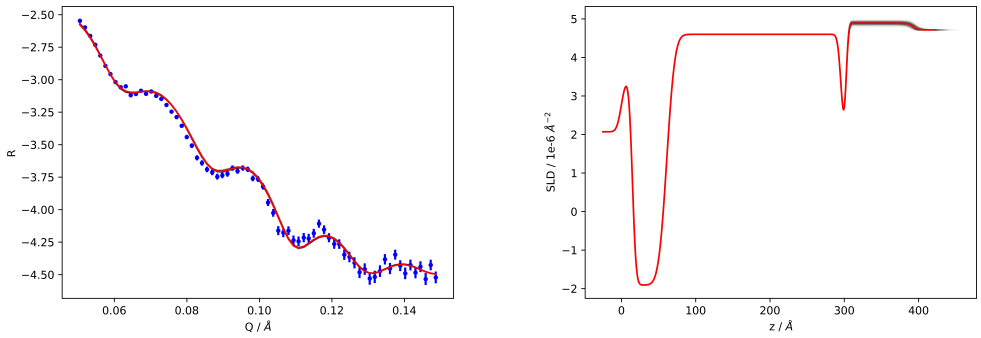

(a) (b)

Fig. S24 Fitting of NR data (blue dots) of PS in the presence of 100 ppm chitosan in GCMW and 100 mM NaCl. The shadowed part indicates the range of possible solutions. a) Fitted curve (red) b) SLD profile.

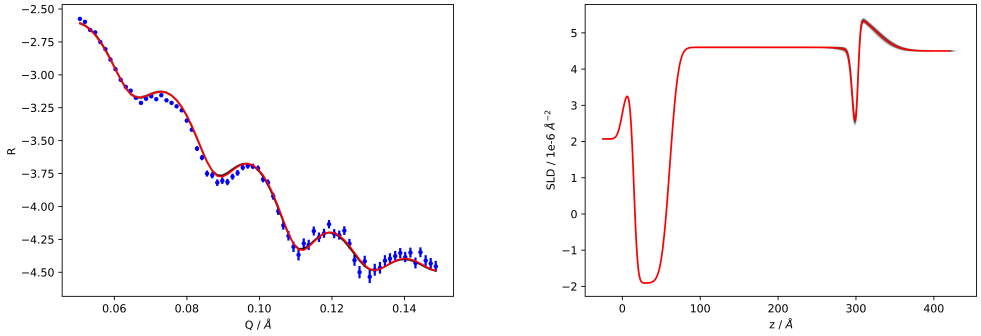

(a) (b)

Fig. S25 Fitting of NR data (blue dots) of PS in the presence of 2 cmc d-SDS after exposure of the surface to chitosan, in GCMW and 100 mM NaCl. The shadowed part indicates the range of possible solutions. a) Fitted curve (red) b) SLD profile.

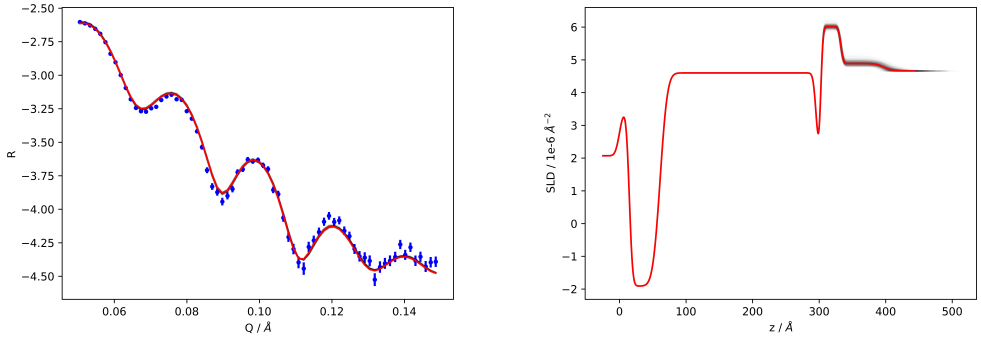

(a) (b)

Fig. S26 Fitting of NR data (blue dots) of PS in the presence of a mixture of 20 cmc d-SDS and 100 ppm chitosan, in GCMW and 100 mM NaCl. The shadowed part indicates the range of possible solutions. a) Fitted curve (red) b) SLD profile.

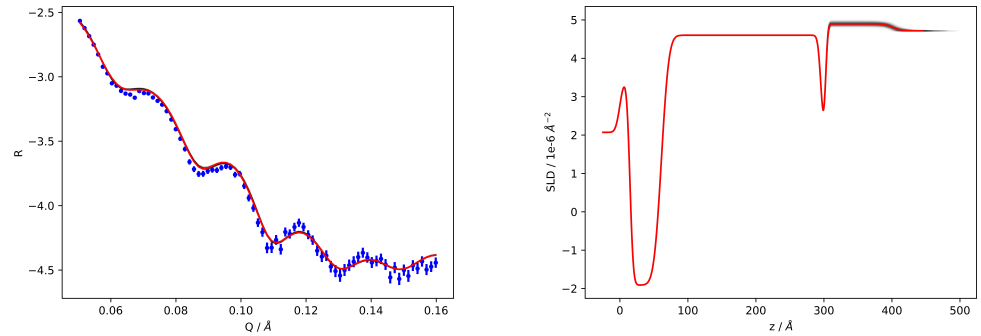

(a) (b)

Fig. S27 Fitting of NR data (blue dots) of PS after rinsing the d-SDS/chitosan mixture with GCMW and 100 mM NaCl. The shadowed part indicates the range of possible solutions. a) Fitted curve (red) b) SLD profile.

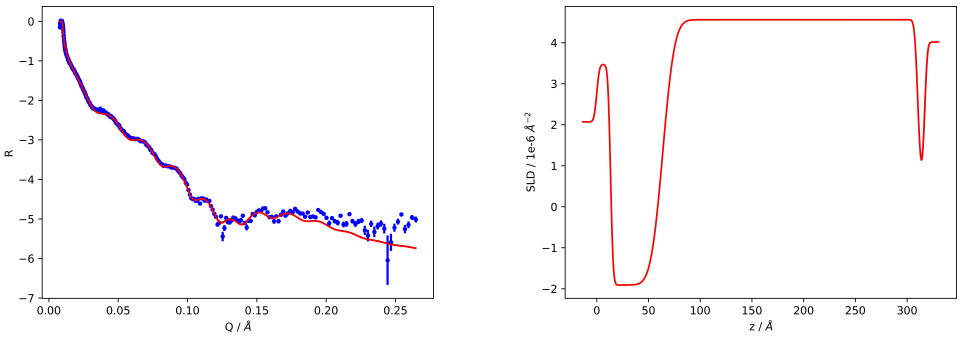

(a) (b)

Fig. S28 Fitting of NR data (blue dots) of PS (sample 2) in GCMW and 100 mM NaCl. The shadowed part indicates the range of possible solutions. a) Fitted curve (red) b) SLD profile.

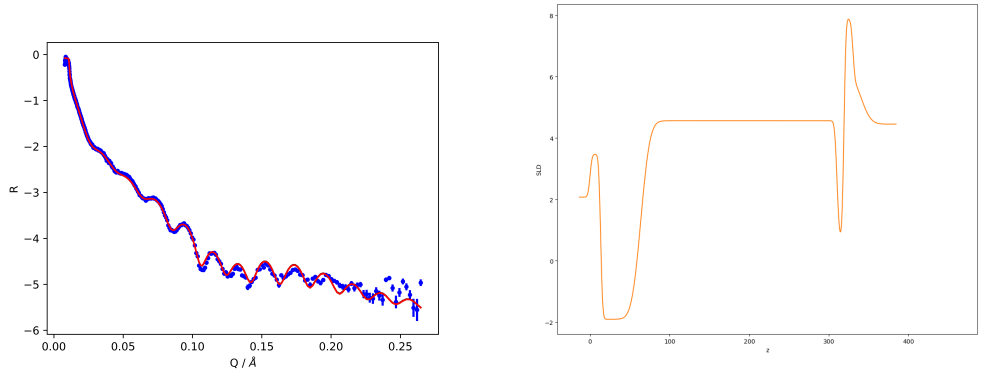

(a) (b)

Fig. S29 Fitting of NR data (blue dots) of PS in the presence of 20 cmc d-SDS in GCMW and 100 mM NaCl. a) Fitted curve (red) b) SLD profile. This fit required a MixedReflectModel as the region of total reflection was lower than 1, suggesting the presence of bubbles. In this case, RefNX can only display the average SLD profile of the main structure.

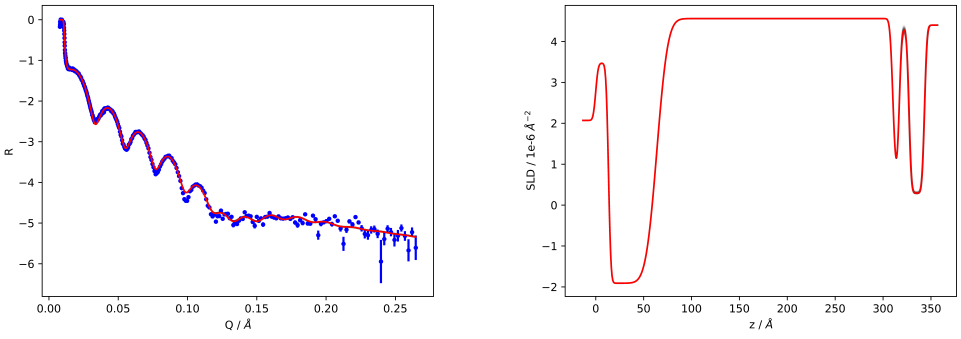

(a) (b)

Fig. S30 Fitting of NR data (blue dots) of PS in the presence of 20 cmc h-SDS in GCMW and 100 mM NaCl. The shadowed part indicates the range of possible solutions. a) Fitted curve (red) b) SLD profile.

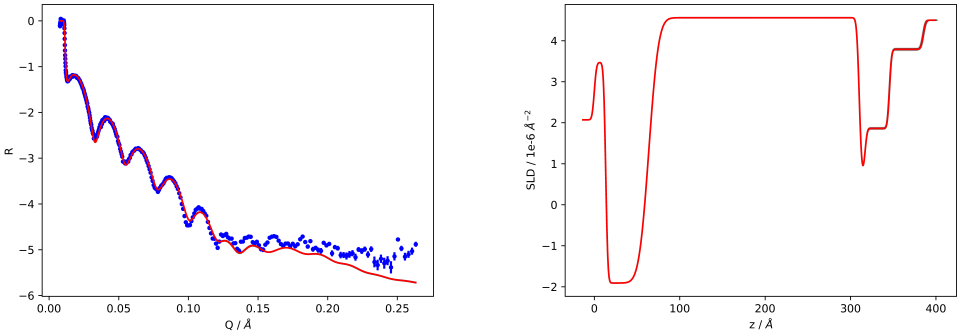

(a) (b)

Fig. S31 Fitting of NR data (blue dots) of PS in the presence of 20 cmc h-SDS and 6 cmc d-TTAB in GCMW and 100 mM NaCl. The shadowed part indicates the range of possible solutions. a) Fitted curve (red) b) SLD profile.

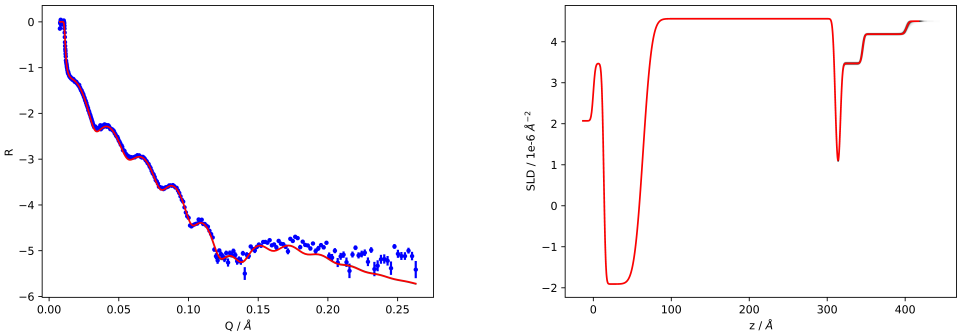

(a) (b)

Fig. S32 Fitting of NR data (blue dots) of PS in the presence of 20 cmc d-SDS and 5.3 mM d-dodecanol in GCMW and 100 mM NaCl. The shadowed part indicates the range of possible solutions. a) Fitted curve (red) b) SLD profile.

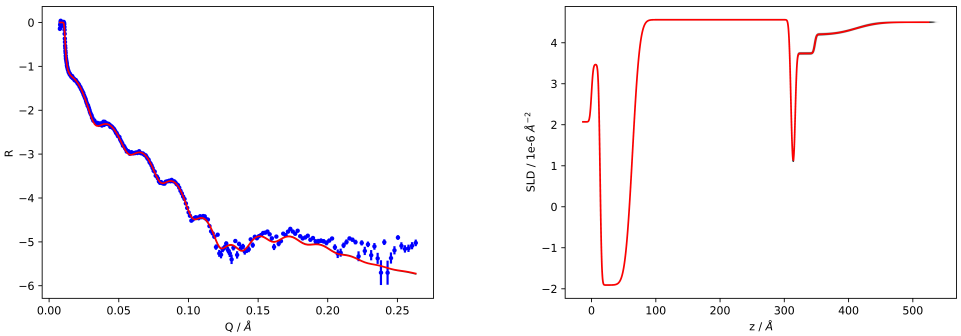

(a) (b)

Fig. S33 Fitting of NR data (blue dots) of PS after rinsing the d-SDS/d-dodecanol mixture in GCMW and 100 mM NaCl. The shadowed part indicates the range of possible solutions. a) Fitted curve (red) b) SLD profile.

Table S2 Bulk SLD values and fitted layer thickness, roughness and SLD values for adsorbed layers on PS surface (sample 1). Numbers in parenthesis indicate the error on the parameter value, equal to 2.5σ. The values in italics were manually adjusted

	bulk SLD ($*10^{-6}$Å^{-2})	SLD ($*10^{-6}$Å^{-2})	Thickness (Å)	Roughness (Å)
2 cmc d-SDS	*4.5*	5.5 (0.2)	28 (10)	23 (4)
20 cmc d-SDS	*4.65*	5.80 (0.06)	34 (1)	3 (2)
100 ppm chitosan	*4.7*	4.88 (0.07)	91 (7)	5 (7)
2 cmc d-SDS after chitosan	*4.7*	5.6 (0.2)	22 (10)	22 (3)
d-SDS/chitosan mixture	*4.66*	6.0 (0.1)	30 (2)	*3*
		4.9 (0.1)	65 (10)	10 (13)
Final rinse	*4.7*	4.9 (0.1)	99 (10)	10 (12)

Table S3 Bulk SLD values and fitted layer thickness, roughness and SLD values for adsorbed layers on PS surface (sample 2). Numbers in parenthesis indicate the error on the parameter value, equal to 2.5σ. The values in italics were manually adjusted

	bulk SLD ($*10^{-6}$Å^{-2})	SLD ($*10^{-6}$Å^{-2})	Thickness (Å)	Roughness (Å)
Thiol layer	*4.01*	0.7 (0.9)	7 (2)	2 (3)
20 cmc d-SDS	*4.45*	0.8 (0.4)	2.0 (0.2)	*2*
		7.99 (0.04)	11.3 (0.6)	*2*
		6.2	10 (1)	9.8 (0.5)
20 cmc h-SDS	*4.4*	4.3 (0.2)	10.1 (0.4)	*2*
		0.29 (0.03)	16.2 (0.4)	2.1 (0.2)
Rinse after h-SDS	*4.5*	3.95 (0.04)	44 (3)	18 (4)
h-SDS/d-TTAB mixture	*4.5*	1.86 (0.02)	28.6 (0.4)	2.02 (0.05)
		3.79 (0.03)	39.5 (0.9)	2.2 (0.7)
Rinse after h-SDS/d-TTAB	*4.5*	0.4 (0.3)	2.6 (0.3)	*2*
		3.60 (0.05)	39 (2)	19.8 (0.8)
h-SDS/d-dodecanol mixture	*4.5*	3.47 (0.03)	28.4 (0.9)	*2*
		4.18 (0.02)	56 (2)	3 (2)
Final rinse	*4.5*	3.74 (0.02)	30 (1)	*2*
		4.20 (0.03)	64 (5)	27 (7)

2.5.2 MBT

Figure S34 shows the reduced data relative to the MBT surface. Figures S35 to S41 show the fitted data in the high Q region (plus low Q region in S41). Corresponding parameters are in Table S4.

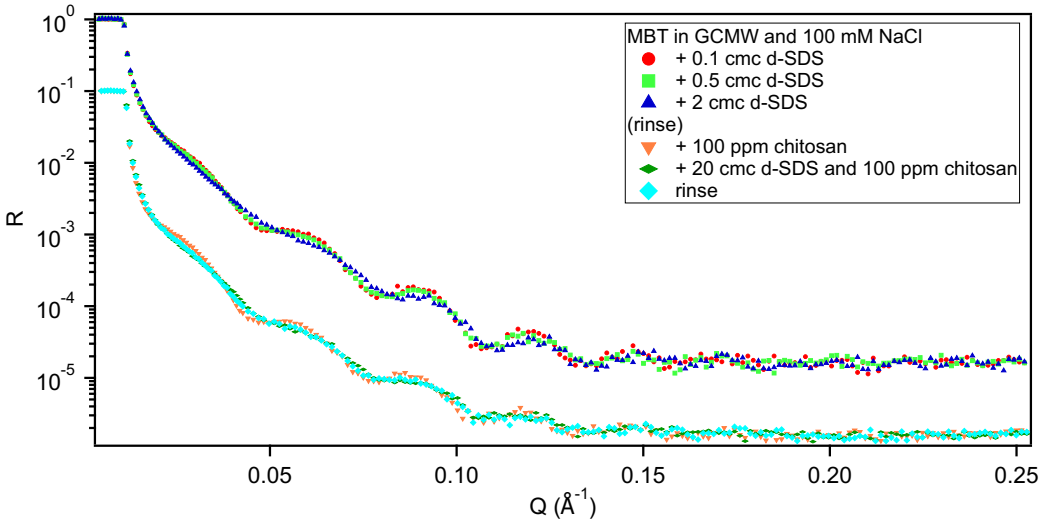

Fig. S34 Reduced NR curves relative to MBT in GCMW and 100 mM NaCl in the presence of the molecules indicated in the graph. The second group of curves is scaled by a factor of 0.1. The step in parenthesis indicates that the surface was rinsed but the measurement was not run due to time constraints.

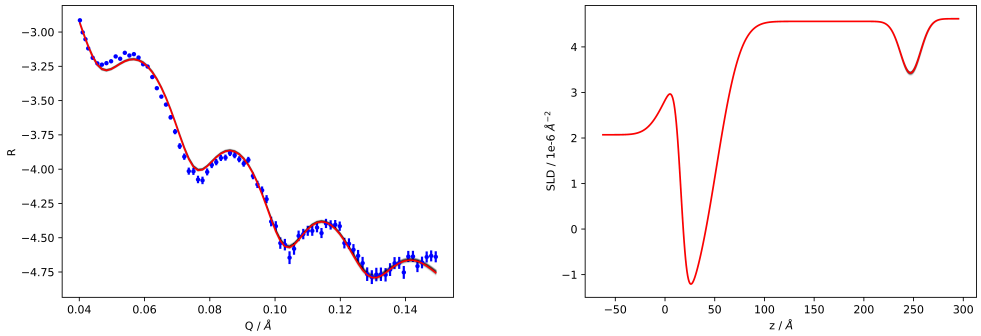

(a) (b)

Fig. S35 Fitting of NR data (blue dots) of MBT (sample 2) in GCMW. The shadowed part indicates the range of possible solutions. a) Fitted curve (red) b) SLD profile.

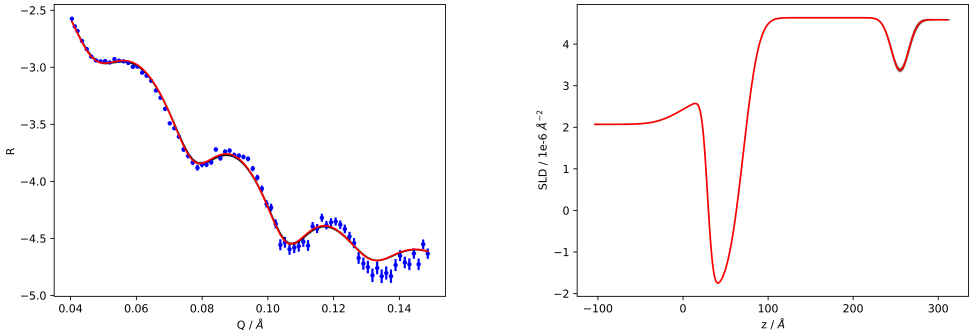

(a) (b)

Fig. S36 Fitting of NR data (blue dots) of MBT in the presence of 0.1 cmc d-SDS in GCMW and 100 mM NaCl. The shadowed part indicates the range of possible solutions. a) Fitted curve (red) b) SLD profile.

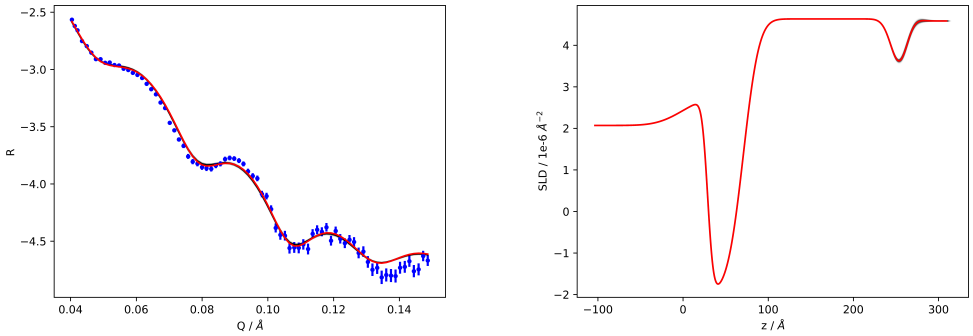

(a) (b)

Fig. S37 Fitting of NR data (blue dots) of MBT in the presence of 0.5 cmc d-SDS in GCMW and 100 mM NaCl. The shadowed part indicates the range of possible solutions. a) Fitted curve (red) b) SLD profile.

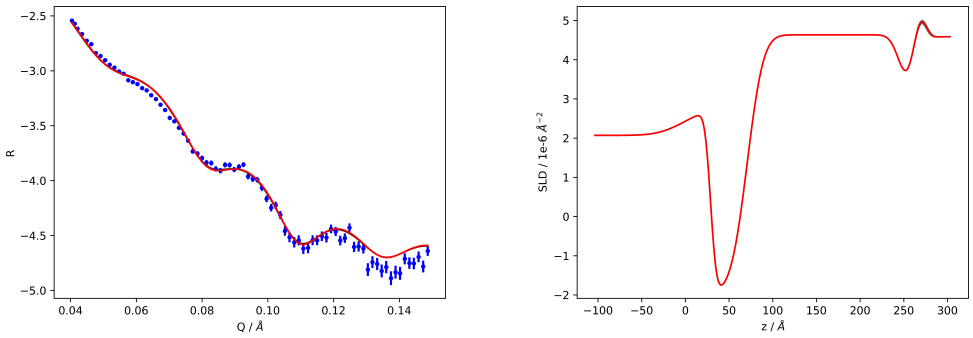

(a) (b)

Fig. S38 Fitting of NR data (blue dots) of MBT in the presence of 2 cmc d-SDS in GCMW and 100 mM NaCl. The shadowed part indicates the range of possible solutions. a) Fitted curve (red) b) SLD profile.

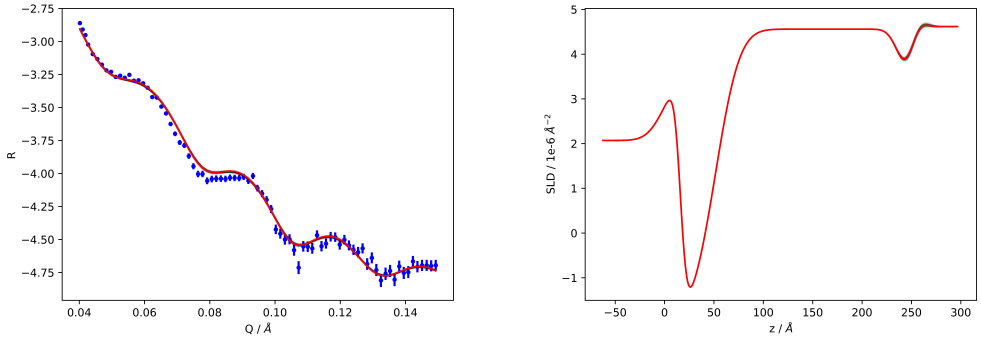

(a) (b)

Fig. S39 Fitting of NR data (blue dots) of MBT in the presence of 2 cmc d-SDS in GCMW. The shadowed part indicates the range of possible solutions. a) Fitted curve (red) b) SLD profile.

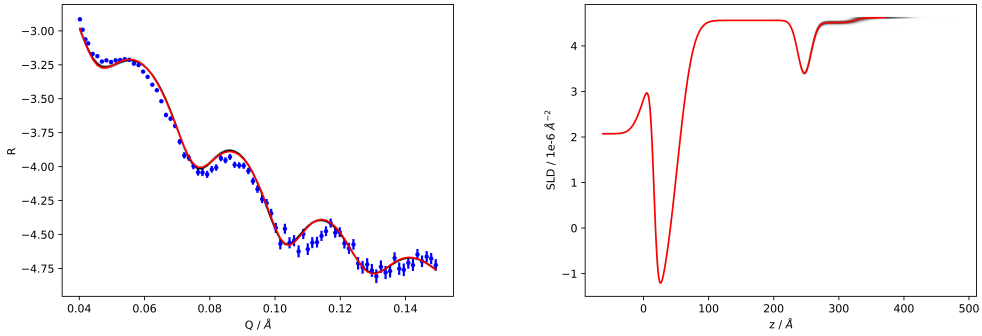

(a) (b)

Fig. S40 Fitting of NR data (blue dots) of MBT in the presence of 100 ppm chitosan in GCMW and 100 mM NaCl. In this case, the fit at low Q resulted in two populations, of thickness ≈ 60 and 250 Å, and undefined SLD. For this reason, the fit at high Q was taken as representative. The shadowed part indicates the range of possible solutions. a) Fitted curve (red) b) SLD profile.

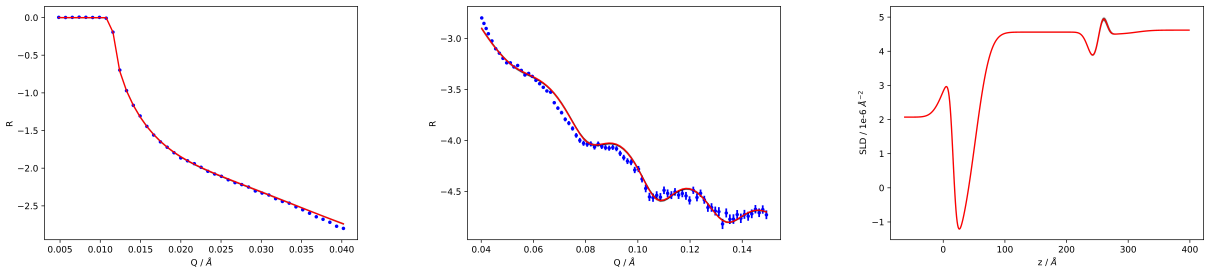

(a) (b) (c)

Fig. S41 Fitting of NR data (blue dots) of MBT in the presence of a mixture of 20 cmc d-SDS and 100 ppm chitosan, in GCMW and 100 mM NaCl. The shadowed part indicates the range of possible solutions. a) Fitted curve (red) at low Q b) fitted curve at high Q c) SLD profile.

Table S4 Bulk SLD values and fitted layer thickness, roughness and SLD values for adsorbed layers on MBT surface. Numbers in parenthesis indicate the error on the parameter value, equal to 2.5σ. The values in italics were manually adjusted

	bulk SLD ($*10^{-6}$Å^{-2})	SLD ($*10^{-6}$Å^{-2})	Thickness (Å)	Roughness (Å)
Thiol layer in GCMW (sample 2)	*4.62*	*-0.25*	6.1 (0.2)	9.98 (0.05)
0.1 cmc d-SDS in 100 mM NaCl	*4.58*	*6.2*	2.2 (0.8)	11 (1)
0.5 cmc d-SDS in 100 mM NaCl	*4.58*	*6.2*	7 (0.5)	9.2 (0.4)
2 cmc d-SDS in 100 mM NaCl	*4.58*	*6.2*	13.8 (0.3)	6 (4)
2 cmc d-SDS in GCMW	*4.62*	*6.2*	10.8 (0.7)	10 (1)
100 ppm chitosan	*4.62*	4.51 (0.05)	76 (17)	10 (14)
d-SDS/chitosan mixture	*4.62*	6.18 (0.04)	13.3 (0.7)	*6*
		4.5	36 (6)	37 (20)

2.5.3 BT

Figure S42 shows the reduced data relative to the BT surface. Figures S43 to S46 show the fitted data in the high Q region (low Q region in S44). Corresponding parameters are in Table S5.

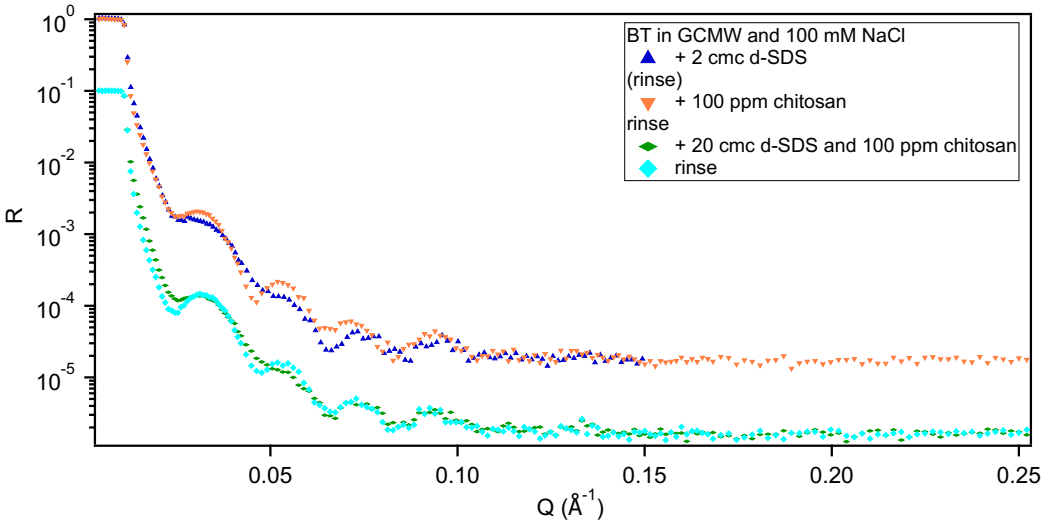

Fig. S42 Reduced NR curves relative to BT in GCMW and 100 mM NaCl in the presence of the molecules indicated in the graph. The second group of curves is scaled by a factor of 0.1. The step in parenthesis indicates that the surface was rinsed but the measurement was not run due to time constraints.

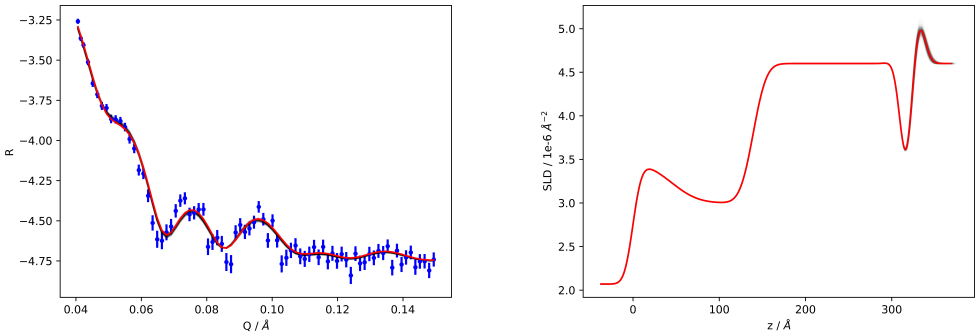

(a) (b)

Fig. S43 Fitting of NR data (blue dots) of BT in the presence of 2 cmc d-SDS in GCMW and 100 mM NaCl. The shadowed part indicates the range of possible solutions. a) Fitted curve (red) b) SLD profile.

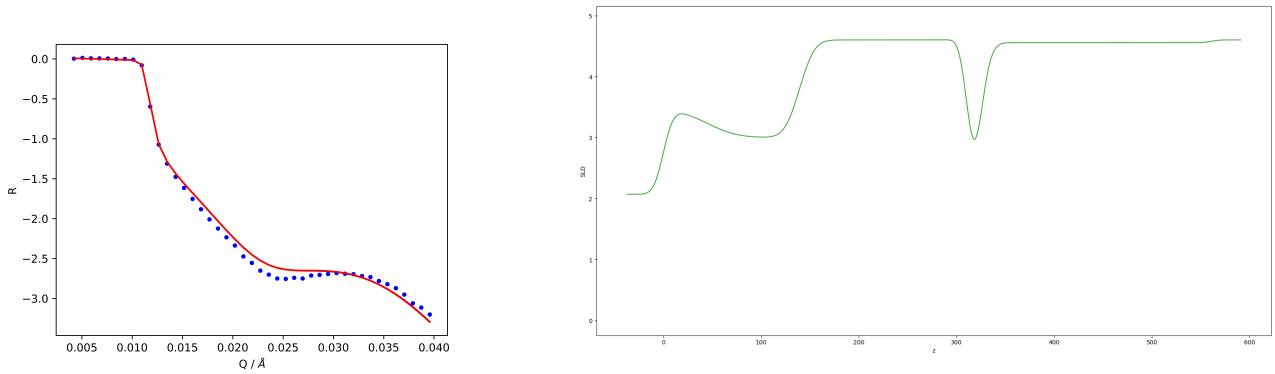

(a) (b)

Fig. S44 Fitting of NR data (blue dots) of BT in the presence of 100 ppm chitosan in GCMW and 100 mM NaCl. a) Fitted curve (red) b) SLD profile. As for Figure S29, a MixedReflectModel was used, and RefNX can only display the average SLD profile of the main structure.

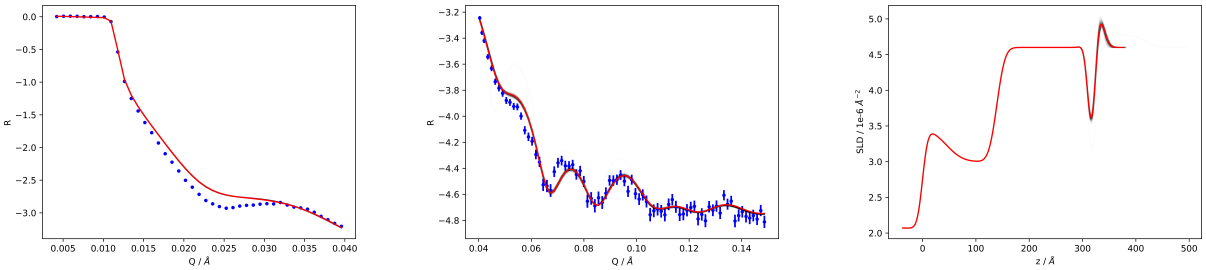

(a) (b) (c)

Fig. S45 Fitting of NR data (blue dots) of BT in the presence of a mixture of 20 cmc d-SDS and 100 ppm chitosan, in GCMW and 100 mM NaCl. The shadowed part indicates the range of possible solutions. a) Fitted curve (red) at low Q b) fitted curve at high Q c) SLD profile.

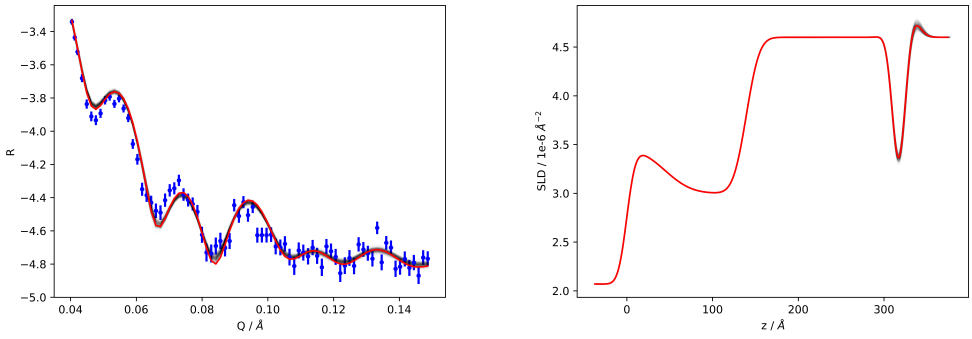

(a) (b)

Fig. S46 Fitting of NR data (blue dots) of BT after rinsing the d-SDS/chitosan mixture with GCMW and 100 mM NaCl. The shadowed part indicates the range of possible solutions. a) Fitted curve (red) b) SLD profile.

Table S5 Bulk SLD values and fitted layer thickness, roughness and SLD values for adsorbed layers on BT surface. Numbers in parenthesis indicate the error on the parameter value, equal to 2.5σ. The values in italics were manually adjusted

	bulk SLD ($*10^{-6}$Å^{-2})	SLD ($*10^{-6}$Å^{-2})	Thickness (Å)	Roughness (Å)
2 cmc d-SDS	*4.6*	*6.2*	14.8 (0.9)	7 (1)
100 ppm chitosan	*4.6*	*4.56*	240 (10)	10 (14)
d-SDS/chitosan mixture	*4.6*	6.18 (0.05)	11 (1)	15.0 (0.1))
		4.56 (0.01)	218 (22)	12 (18)
Final rinse	*4.6*	5.6 (0.2)	14 (3)	*9*

3 Quartz-crystal Microbalance (QCM)

Quartz-crystal microbalance is a useful technique to study the adsorption process in a wide range of cases. The sensor is a quartz crystal with a specific resonance frequency. By applying a voltage to the electrodes on the crystal, it oscillates, and if molecules adsorb on top of the crystal, its resonance frequency changes. The QCM instrument monitors this frequency shift to gain information about the mass adsorbed on the surface. In the simplest case, the two parameters (frequency shift Δf and adsorbed mass Δm) are related by the Sauerbrey equation $\Delta m = -C * \Delta f / n$, where C is a constant depending on the crystal and n is the overtone number[3]. A QCM instrument, in fact, monitors the fundamental frequency plus its overtones from n=3 to n=13. It can also monitor the energy dissipated during the adsorption process (QCM-D, quartz-crystal microbalance with dissipation monitoring). This adds information on the mechanical properties of the adsorbed layer. Often, the frequency shift is due not only to mass adsorption but also to changes in the viscoelastic properties of the system. In this case, the Sauerbrey equation fails and more complex models are needed to analyse the recorded signal (for a complete description, see[4] and references therein).

This is the case with the systems presented here. QCM-D was used mainly to investigate further the unexpected adsorption of SDS on the negatively charged PS surface. Measurements were performed on a Q-Sense Analyser (Biolin Scientific), using a gold-coated quartz crystal with a resonance frequency of 5 MHz (OpenQCM). The crystal was cleaned by UV/ozone treatment followed by sonication in solvents of increasing polarity. It was then mounted in the QCM cell and functionalized *in situ* injecting a 1 mM solution of PS in absolute ethanol, and incubating for 20 h. The cell was then rinsed with ethanol to remove the excess physisorbed thiol, and subsequently a 100 mM NaCl solution in MilliQ water was introduced to obtain the baseline for the adsorption measurement. The applied sequence was the same as for the NR experiments, but hydrogenous SDS was used instead of the deuterated one. The steps are then: 2 cmc h-SDS, 20 cmc h-SDS, rinse, 100 ppm chitosan, 2 cmc h-SDS, mixture of 20 cmc h-SDS and 100 ppm chitosan, rinse. The solutions, previously degassed, were fluxed at 100 μL/min until a plateau was reached (15-30 min). The full measurement is shown in Figure S47. The fundamental frequency, as often happens, was very noisy so it is not included in the graph.

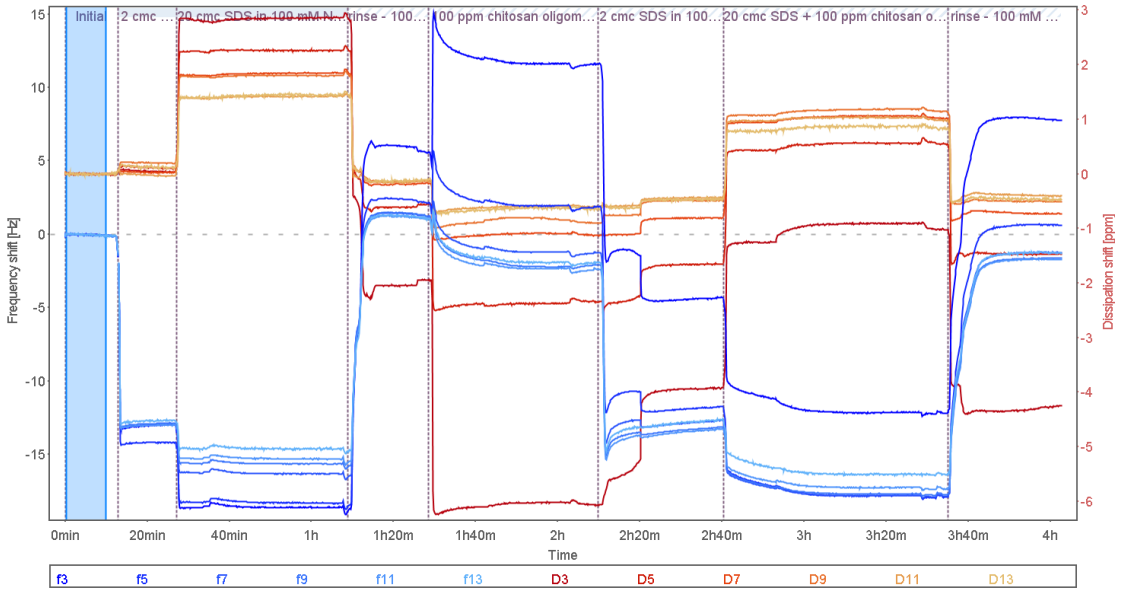

Fig. S47 QCM-D measurement for the adsorption on PS of: 2 cmc SDS, 20 cmc SDS, 100 ppm chitosan, 2 cmc SDS after exposure to chitosan, a mixture of 20 cmc SDS and 100 ppm chitosan, with rinses in between. Blue, frequency shifts. Red, dissipation. Overtones from 3 (darker colours) to 13 (lighter colours) are shown.

In the case of 20 cmc h-SDS, 100 ppm chitosan and their mixture, after 15 min the flux was stopped and the solution incubated for ca. 30 min. This explains the steps visible in the graph in the presence of these solutions, but not the one appearing when fluxing 2 cmc h-SDS after chitosan. Also, overtones are spread out and some frequency shifts are positive, the most striking example being f3 after injection of chitosan. A positive Δf indicates mass loss for homogeneous rigid layers, but it can also be explained by a change in the mechanical properties of the adsorbed layer, i.e., adsorption of a softer layer[4,5]. When h-SDS is injected after chitosan, higher overtones are at about the same level as previously, and the same is true for the mixture containing 20 cmc h-SDS, but the variations in dissipation suggests that the properties of the adsorbed layer are different, and this is likely due to chitosan. As overtones probe different distances towards the bulk (their penetration depth is inversely proportional to the overtone number[6,5]), chitosan is probably mainly distributed in a second layer further from the surface, while the first layer may be more rigid (low dissipation for higher overtones). The adsorbed layers are probably not completely removed by the final rinse, considering the spreading in the overtones at the end of the measurement. The qualitative conclusions drawn here are in line with the NR data presented in this paper and are supported by literature findings on

QCM on polysaccharides or polyelectrolyte/surfactant mixtures (see e.g.[7 8 9]). Dhopatkar *et al.*, interestingly, suggest a two-layer model for adsorption of polyelectrolyte/surfactant mixtures, where the first layer has an elastic behaviour and is not removed by rinsing, while the second one is viscous and loosely adsorbed[8].
The data was plotted and tentatively analysed using the software QSense Dfind (Biolin Scientific). Dfind has two models for viscoelastic modeling: Smartfit and Broadfit. The first one returns two solutions, on the assumption that the adsorbed layer is either thin and rigid or thick and soft. The latter has one solution, found by looking for the best fit at each point independently. Unfortunately the models failed for such a complex sequence. The measurement was repeated, functionalizing two new gold-coated crystals (Biolin Scientific), *ex situ*, by immersing one in a 1 mM PS solution and the other in a 1 mM MBT solution. The QCM measurement was then run in parallel on the two to compare the effect of surface charge on h-SDS adsorption. Results are in Figure S48.

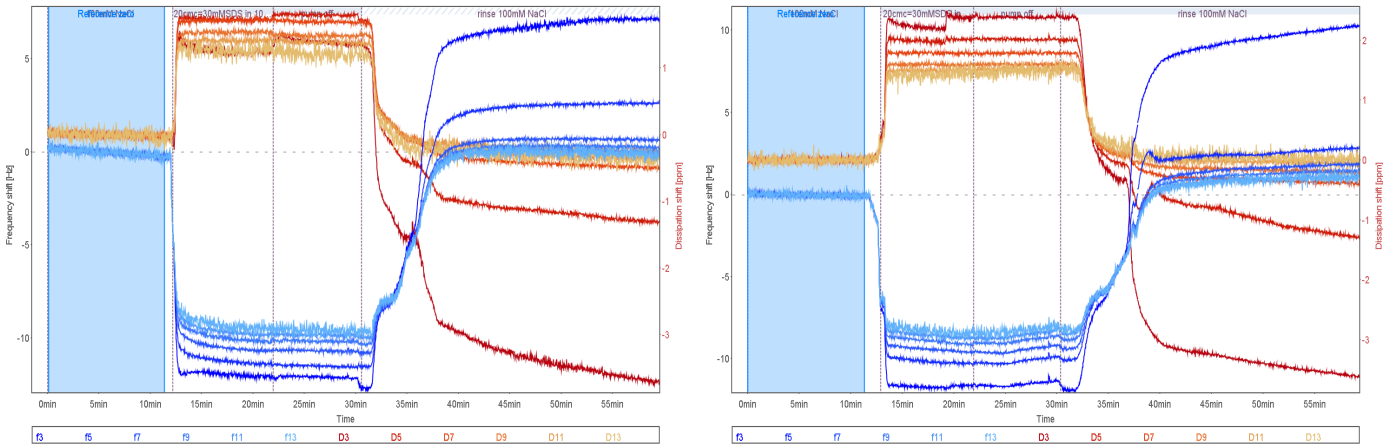

(a) (b)

Fig. S48 QCM-D measurement for the adsorption of a 20 cmc h-SDS solution in 100 mM NaCl on a) PS, and b) MBT. Blue, frequency shifts. Red, dissipation. Overtones from 3 (darker colour) to 13 (lighter colour) are shown.

Both have been analysed applying both Broadfit and Smartfit models. It was considered, though, that most of the adsorbed species is likely to be dodecanol, as h-SDS was used without further purification. In the case of the PS surface, both models show a good fit quality and the solution found by Broadfit agrees with the second Smartfit solution, suggesting a soft adsorbed layer. Instead, when fitting MBT data, Broadfit and the first Smartfit solution converge, suggesting a rigid layer (Figure S49). The adsorbed mass is ca. 200 ng/cm^2 on PS, and ca. 400 ng/cm^2 on MBT. These results agree with NR ones, that indicate a more compact adsorbed layer on hydrophobic surfaces.

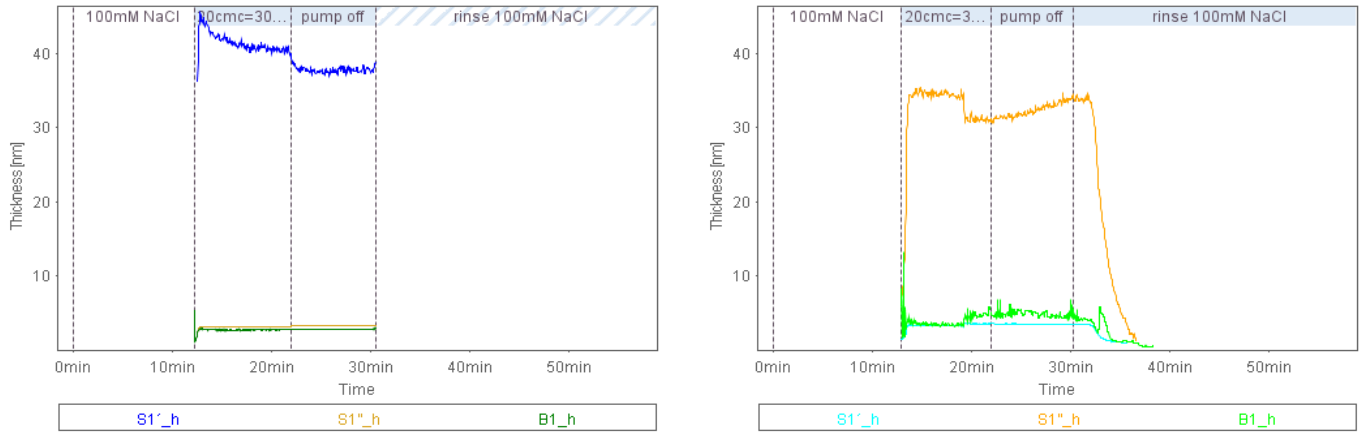

(a) (b)

Fig. S49 Fitting of QCM-D measurement for the adsorption of a 20 cmc h-SDS solution in 100 mM NaCl on a) PS, and b) MBT. Smartfit solutions S1' and S1" are in (light) blue and orange, respectively, Broadfit solution B1 is in green.

Notes and references

1 T. A. Darwish, N. R. Yepuri, P. J. Holden and M. James, *Analytica Chimica Acta*, 2016, **927**, 89–98.

2 *https://github.com/Alexey-Klechikov/pySAred*.

3 G. Sauerbrey, *Zeitschrift für Physik*, 1959.

4 I. Reviakine, D. Johannsmann and R. P. Richter, *Analytical Chemistry*, 2011, **83**, 8838–8848.

5 G. A. McCubbin, S. Praporski, S. Piantavigna, D. Knappe, R. Hoffmann, J. H. Bowie, F. Separovic and L. L. Martin, *European Biophysics Journal*, 2011, **40**, 437–446.

6 M. Rodahl and B. Kasemo, *Sensors and Actuators A: Physical*, 1996, **54**, 448–456.

7 A. Tiraferri, P. Maroni, D. Caro Rodríguez and M. Borkovec, *Langmuir*, 2014, **30**, 4980–4988.

8 N. Dhopatkar, J. H. Park, K. Chari and A. Dhinojwala, *Langmuir*, 2015, **31**, 1026–1037.

9 M. Hernández-Rivas, E. Guzmán, L. Fernández-Peña, A. Akanno, A. Greaves, F. Léonforte, F. Ortega, R. G. Rubio and G. S. Luengo, *Colloids and Interfaces*, 2020, **4**, 33.